

Spatiotemporal variability of soil respiration in a seasonal tropical forest

Vanessa E. Rubio^{1,2}  | Matteo Detto^{1,3}

¹Smithsonian Tropical Research Institute, Balboa, Panama

²Department of Biological Sciences, University of Los Andes, Bogota, Colombia

³Department of Ecology and Evolutionary Biology, Princeton University, Princeton, NJ, USA

Correspondence

Vanessa E. Rubio, Smithsonian Tropical Research Institute, Balboa, Panama.
Email: v.rubio3403@uniandes.edu.co

Abstract

We monitored soil CO₂ effluxes for over 3 years in a seasonally wet tropical forest in Central Panama using automated and manual measurements from 2013 to 2016. The measurements displayed a high degree of spatial and temporal variability. Temporal variability could be largely explained by surface soil water dynamics over a broad range of temporal scales. Soil moisture was responsible for seasonal cycles, diurnal cycles, intraseasonal variability such as rain-induced pulses following dry spells, as well as suppression during near saturated conditions, and ultimately, interannual variability. Spatial variability, which remains largely unexplained, revealed an emergent role of forest structure in conjunction with physical drivers such as soil temperature and topography. Mean annual soil CO₂ effluxes (\pm SE) amounted to 1,613 (\pm 59) gC m⁻² year⁻¹ with an increasing trend in phase with an El Niño/Southern Oscillation (ENSO) cycle which culminated with the strong 2015–2016 event. We attribute this trend to a relatively mild wet season during which soil saturated conditions were less persistent.

KEYWORDS

automated and manual chamber, El Niño/Southern Oscillation, forest structure, spatial and temporal variability

1 | INTRODUCTION

Tropical forests contribute to the global carbon cycle through storing 40% of global terrestrial carbon stocks (Beer et al., 2010; Jobbágy & Jackson, 2000; Pan et al., 2011), 56% of which, is found in aboveground biomass and 32% in soils (Ngo et al., 2013; Pan et al., 2011). For their major role in the global carbon cycle, they will strongly influence future concentrations of atmospheric carbon dioxide (Cox et al., 2013; Sayer, Heard, Grant, Marthews, & Tanner, 2011).

Carbon assimilated by the biosphere is released through autotrophic and heterotrophic respiration (Malhi et al., 1998; Trumbore, 2006) of which respiration from soils is the major component, and second in magnitude only to gross primary productivity (Raich & Schlesinger, 1992). However, the spatial distribution of this carbon source and its sensitivity to global climate change are still uncertain (Pendall et al., 2004), especially in the tropics (Cavaleri, Reed, Smith, & Wood, 2015).

Quantifying the spatial and temporal variability of soil respiration is necessary to estimate ecosystem carbon losses at regional and global scale, and in understanding the mechanisms that control such losses (Phillips et al., 2017), yet, it remains a major challenge (Houghton, 2005; Metcalfe et al., 2007; Schwendenmann & Veldkamp, 2006). Soil is a complex and spatially heterogeneous mixture of minerals and organic pools, including litter, roots, and microorganisms. Each of these components responds differently to environmental variability (Li, Yang, & Fang, 2013) and are uniquely coupled with other biotic processes, such as nutrient recycling (Sayer et al., 2011), generating a broad spectrum of CO₂ emission rates. It is not surprising that soil respiration rates in tropical forests vary considerably (Table 1), comprising from 41% to 44% (Chambers et al., 2004; Malhi, Doughty, & Galbraith, 2011), up to 60%–80% of the total ecosystem respiration (Goulden, Munger, Fan, Daube, & Wofsy, 1996; Raich & Schlesinger, 1992; Wofsy et al., 1993).

This is an open access article under the terms of the Creative Commons Attribution License, which permits use, distribution and reproduction in any medium, provided the original work is properly cited.

© 2017 The Authors. *Ecology and Evolution* published by John Wiley & Sons Ltd.

TABLE 1 Mean annual soil CO₂ efflux (gC m⁻² year⁻¹) in different tropical forests around the world. The annual budgets were computed from the mean soil CO₂ efflux reported in the study, converted in μmol m² s⁻¹ and multiplied by 12 × 10⁻⁶ × 3,600 × 24 × 365. The length of the study period and the method are also indicated

References	Location	Period	Ecosystem type	Efflux	Method
Wood et al. (2013)	Luquillo, Puerto Rico	6 months	Subtropical wet forest	4,352	Automated chamber IRGA
Valentini et al. (2008)	Northwest Mato Grosso, Brazil	11 months	Upland tropical forest	2,887	Dynamic closed chamber IRGA
Vargas and Allen (2008)	Northeast Yucatan Peninsula, Mexico	16 months	Dense, even-aged tropical forest	2,876	Solid-state CO ₂ sensors
Malhi et al. (1998)	Cuieiras, near Manaus, Brazil	1 year	Lowland terra firme tropical rainforest	2,649	Edisol eddy covariance system IRGA
Sotta (1998)	Manaus, Brazil	2 months	Terra firme wet tropical forest	2,596	Dynamic closed chamber IRGA
Hashimoto et al. (2004)	Chiang-Mai, Northern Thailand	2 years	Hill evergreen tropical forest	2,560	Portable closed chamber IRGA
Sotta et al. (2004)	Manaus, Brazil	6 months	Lowland terra firme rainforest	2,441	Dynamic open chamber IRGA
Takahashi et al. (2011)	Kanchanaburi province, Western Thailand	3 years	Seasonal tropical forest (lower slope)	2,343	Static closed chamber IRGA
Katayama et al. (2009)	Sarawak, Malaysia	4.6 years	Lowland mixed-dipterocarp forest	2,214	Dynamic closed chamber IRGA
Ohashi, Kume, Yamane, and Suzuki (2007)	Sarawak, Malaysia	22 months	Primary tropical rainforest	2,013	Dynamic closed chamber IRGA
Adachi, Bekku, Rashidah, Okuda, and Koizumi (2006)	Malaysian Peninsula	2 days	Secondary tropical forest	2,002	Portable closed chamber IRGA
Davidson et al. (2000)	Paragominas, Brazil	15 months	Primary tropical forest	2,000	Dynamic closed chamber IRGA
Adachi et al. (2006)	Malaysian peninsula	2 days	Primary tropical forest	1,985	Portable closed chamber IRGA
Adachi et al. (2005)	Negeri Sembilan, Malaysia	2 days	Primary tropical forest	1,837	Portable system IRGA
Ibañez, (2015)	Nyungwe forest, Rwanda	6 months	Secondary tropical mountain rainforest	1,830	Dynamic closed chamber IRGA
Davidson et al. (2000)	Paragominas, Brazil	1.25 years	Secondary tropical forest	1,800	Dynamic closed chamber IRGA
Adachi, Ishida, Bunyavejchewin, Okuda, and Koizumi (2009)	Western Thailand	2.5 years	Seasonally tropical dry forest	1,724	Portable closed chamber IRGA
Kosugi et al. (2007)	Malaysian peninsula	3 years	Primary lowland mixed dipterocarp forest	1,703	Dynamic closed chamber IRGA
Takahashi et al. (2011)	Kanchanaburi province, Western Thailand	3 years	Seasonal tropical forest (ridge)	1,701	Static closed chamber IRGA
Metcalfe et al. (2007)	Pará State, Brazil	1 year	Lowland terra firme rainforest (Fertile site)	1,699	Dynamic open chamber IRGA
Adachi et al. (2005)	Negeri Sembilan, Malaysia	2 days	Secondary tropical forest	1,691	Portable system IRGA
Zhou et al. (2013)	Southwest of Hainan Island, China	2 years	Primary tropical forest	1,673	Automated closed chamber IRGA
This study	BCI, Panama	3 years	Lowland tropical forest	1,613	Dynamic closed chamber IRGA
Epron et al. (2006)	French Guiana	1 month	Lowland terra firme rain forest	1,612	Dynamic closed chamber IRGA
Ibañez, (2015)	Nyungwe forest, Rwanda	6 months	Primary tropical mountain rainforest	1,570	Dynamic closed chamber IRGA

(Continues)

TABLE 1 (Continued)

References	Location	Period	Ecosystem type	Efflux	Method
Jiang et al. (2016)	Southwest of Hainan Island, China	3 years	Primary mountain rainforest	1,567	Automated closed chamber IRGA
Zhou et al. (2013)	Southwest of Hainan Island, China	2 years	Secondary tropical forest	1,510	Automated closed chamber IRGA
Kursar (1989)	BCI, Panama	2 years	Lowland tropical forest	1,506	Chamber-syringe/Dynamic close chamber IRGA
Sotta et al. (2006)	Pará State, Brazil	2 years	Lowland terra firme rainforest (sandy soil)	1,487	Dynamic closed chamber IRGA
Wu, Goldberg, Mortimer, and Xu (2016)	Yunnan Province, China	1 year	Secondary forest	1,457	Dynamic closed chamber IRGA
Schwendenmann et al. (2003)	La Selva, Costa Rica	2 years	Tropical wet forest (residual soil)	1,425	Dynamic closed chamber IRGA
Giardina et al. (2014)	Mauna Kea Volcano, Hawaii	11 months	Tropical montane wet forest	1,390	Dynamic closed chamber IRGA
Schwendenmann and Veldkamp (2006)	La Selva, Costa Rica	5 years	Tropical wet forest (residual soil)	1,381	Dynamic closed chamber IRGA
Malhi et al. (2011)	–	–	–	1,350	–
Jiang et al. (2016)	Southwest of Hainan Island, China.	3 years	Secondary mountain rainforest	1,300	Automated closed chamber IRGA
Schwendenmann and Veldkamp (2006)	La Selva, Costa Rica	5 years	Tropical wet forest (old alluvium soil)	1,211	Dynamic closed chamber IRGA
Chambers et al. (2004)	Manaus, Brazil	1 year	Old-growth closed canopy terra firme	1,211	Dynamic closed chamber IRGA
Sotta et al. (2006)	Pará State, Brazil	2 years	Lowland terra firme rainforest (clay soil)	1,166	Dynamic closed chamber IRGA
Schwendenmann et al. (2003)	La Selva, Costa Rica	2 years	Tropical wet forest (old alluvium soil)	1,077	Dynamic closed chamber IRGA
Li et al. (2006)	Luquillo, Puerto Rico	7 months	Secondary wet tropical forest	1,048	Alkali trap method
Sayer et al. (2011)	Gigante, Panama	1 year	Lowland tropical forest	1,000	Dynamic closed chamber IRGA
Fernandes, Bernoux, Cerri, Feigl, and Piccolo (2002)	Rondonia State, Brazil	1 year	Open humid tropical forest	984	Chamber-syringe method
Kiese and Butterbach-Bahl (2002)	Queensland, Australia	4 years	Tropical rainforest	835	Automated chamber IRGA
Sha et al. (2005)	Xishuangbanna, China	1 year	Tropical rainforest	831	Static opaque chamber (chromatography)
La Scala, Marques, Pereira, and Corá (2000)	Sao Pablo, Brazil	3 days	Tropical bare soil	792	Dynamic closed chamber IRGA
Mo et al. (2007)	Guangdong Province, Southern China	1 year	Old-growth monsoon evergreen forest	604	Static chamber (chromatography)

Climatic factors such as precipitation and radiation largely drive temporal variability in soil respiration, influencing soil moisture, temperature, and many biotic processes such as root, soil microbes, and litterfall dynamics. Wet and moist tropical climates are characterized by intense and frequent rainfall events, with or without a seasonal cycle. Soil moisture is probably the most important abiotic factor influencing soil respiration within tropical forests (e.g., Li, Xu, & Zou, 2006; Sotta et al., 2006). Soil CO₂ efflux can be suppressed in both low and high soil water content (Davidson, Belk, & Boone, 1998; Linn & Doran, 1984). High water content creates a barrier to gas diffusion at the

soil-atmosphere interface, limiting the escape of CO₂ and supply of oxygen (Liptzin, Silver, & Detto, 2010), thereby reducing both, production and diffusion of CO₂ (Davidson, Samanta, Caramori, & Savage, 2012; Fang & Moncrieff, 1999). At low soil moisture conditions, decomposition is limited by soluble carbon availability (Davidson et al., 2012; Linn & Doran, 1984).

Several nonlinear relationships have been proposed to link soil respiration rate and soil water content (Cook & Orchard, 2008; Davidson, Verchot, Cattanio, Ackerman, & Carvalho, 2000), indicating optimal conditions for microbial decomposition and root respiration

at intermediate moisture conditions. However, these relationships remain empirical, and it is unknown how they vary with soil, climate, and forest type. In addition, these relationships can be altered during rain-induced pulses, which can be caused by large amounts of water-soluble carbon leaching from the litter or dead microbes, accumulated during dry periods, known as the “Birch effect.” Although these pulses are often observed in dry ecosystems (Ma, Baldocchi, Hatala, Detto, & Yuste, 2012), are less documented in tropical forests (Cleveland & Townsend, 2006). Because this nonmonotonic and nonlinear response, the effect of changing in rainfall variability is difficult to predict in a particular forest without available observations.

In contrast, soil temperature fluctuations in the tropics are small, especially in areas covered by dense vegetation, where little radiation reaches forest floors. Although temperature is a direct factor affecting root and microbes metabolic rates (Kuzakov & Gavrichkova, 2010; Lükewille & Wright, 1997) and is responsible for the temporal variation in soil respiration, primarily in temperate (e.g., Hanson, Wullschleger, Bohlman, & Todd, 1993; Vargas, Detto, Baldocchi, & Allen, 2010) and boreal ecosystems (Shibistova et al., 2002), it might play a secondary role in tropical forests (Davidson et al., 2000). For example, results from a rain exclusion plots suggest that the positive effect of temperature on soil CO₂ efflux is still constrained by soil moisture availability (Wood, Detto, & Silver, 2013).

Relative to temporal variability, spatial variability is less understood, and it can be driven by heterogeneity in below ground physical, chemical, and biological soil properties, landforms, and vegetation cover (Hanson et al., 1993; Xu & Qi, 2001). Spatial variability is also known to be very large at small scales (Epron, Bosc, Bonal, & Freycon, 2006; Kursar, 1989). By shielding intercepting rainfall and determining root distribution, above ground forest structure can create microheterogeneity in the physical and biotic drivers of soil respiration (Raich & Tufekcioglu, 2000). Species composition may also play an important role, as plant species differ in the production and quality of detritus (Raich & Tufekcioglu, 2000), root system, and associations with microorganisms such as fungi and bacterial communities (Barberán et al., 2015). Plant-soil feedbacks have an important role in the ecosystem nutrient cycling and soil carbon exchange through productivity and carbon input into the soil (Balogh et al., 2011; Bardgett, Freeman, & Ostle, 2008; Sayer et al., 2011). For example, diurnal fluctuations in soil CO₂ effluxes may also be caused by translocation of photosynthates from leaves to roots (Detto et al., 2012; Kuzakov & Gavrichkova, 2010).

At larger scales, topographic features (slopes, plateau, and valley) influence hydrological processes and determine heterogeneity in water availability, soil texture, and nutrients (Silver, Scatena, Johnson, Siccama, & Sanchez, 1994; Weintraub et al., 2015). However, the effects on soil respiration are still unclear and literature reports mixed results. Sotta et al. (2006) and Hanson et al. (1993) found no differences between landforms in the Eastern Amazonia and South East US, respectively, while other studies found strong relationship between soil respiration and topographic position, decreasing from hills to bottomlands (Chambers et al., 2004; Epron et al., 2006) or increasing from ridge to lower slopes (Takahashi et al., 2011).

The spatiotemporal variability complicates ground-based monitoring of soil respiration because of the inherent trade-off between temporal and spatial sampling resolution. Recent advances in automated systems have greatly improved our ability to monitor temporal variability up to a half hourly resolution, which is comparable to the scale of variation of many climatic and hydrological drivers. However, systems such as dynamic chambers rely on a centralized gas sampling design, which limits their applications in spatially heterogeneous environments. Manual measurements are more adaptable to spatially stratified sampling designs, but sampling frequency is often insufficient to resolve all scales of variation, and there are other logistic problems limiting sampling at night or during, and immediately after rain events. A combination of manual and automated measurements could provide sufficient information to accurately quantify the soil CO₂ effluxes. Unfortunately, tropical studies that integrate this approach on a sufficiently large temporal horizon are scant (see Table 1).

The objectives of this study were to quantify soil respiration in a lowland seasonally wet tropical forest and analyze their spatial and temporal variability. We used both, manual and automated systems, collecting more than three years of measurements, which include a strong El Niño event. In particular, we investigated the effects of soil moisture, soil temperature, topography, and forest structure. Finally, in order to compute integrated seasonal and annual budgets, we assimilated the measurements in a statistical model at daily scale using Artificial Neural Network.

2 | METHOD

2.1 | Site description

The study site is located on Barro Colorado Island (BCI), Panama (9°9'N, 79°50' W), a 15 km² island in the middle of the Lake Gatun. The forest is tropical moist with a distinct dry season between January and April. Mean annual temperature is 27°C, with minimal seasonal variation; mean annual rainfall is 2642 (±566) mm.

The study was conducted in 6 ha plot at 140 m.a.s.l. on the island plateau. Soil is oxisol containing mainly red light clays, with the majority freely drained, but restricted subsoil permeability giving temporary ponding (Baillie, Elsenbeer, Barthold, Grimm, & Stallard, 2005; Windsor, 1990). The canopy is generally 20–40 m tall estimated to hold 281±20 Mg/ha of aboveground biomass, lianas included (Leigh et al., 2004). In the study plot, The tree density (dbh > 100 mm) at the plot is 287 stem/ha with *Gustavia superba*, *Alseis blackiana*, *Trichillia tuberculata*, *Spondias radlkoferi*, *Luehea seemannii*, and *Hura crepitans*, as the most common species.

2.2 | Automated dynamic chamber system

An automated CO₂ chamber system (LI8100, Licor Bioscience) was installed from June 2013 until January 2015 and from April 2016 to end of August 2016. The system included four automated Dynamic and automatic closed chamber, a multiplexer and a close-path infrared gas analyzer. Each chamber operated every 20 min and CO₂

concentration measurements were taken every second for 2 min after the chamber was closed. A 30-sec prepurge and 45-s postpurge were introduced to allow flushing the system between each measurement.

The soil collars had an outside diameter of 11.4 cm and were installed 5 cm into the soil 1 month before measurements commenced. The collars were located at the vertices of a 20 × 20 m square centered at the microclimatic tower, where power grid was available.

Data collection was interrupted few times due to power losses (about 33 days total). On May 2014, the pump failed and the sensor was sent for repair and factory recalibration; it was reinstalled on July 2014 until January 2015, when it was designated to another experiment. A new, factory calibrated, identical system was installed in April 2016. The automated system had been operative for 617 days, during which it was visited regularly every 1–2 weeks to check the operative status and clean the chambers from litter or other debris that could prevent perfect closure.

2.3 | Portable static chamber system

In May 2013, we installed 27 polyvinyl chloride plastic (PVC) rings (25 cm of diameter), inserted at 5 cm of depth and distributed in two different topographic features, plateau and slope, spaced approximately 20 m across the plot (Fig. S1) 1 month before measurements commenced. On August 2014, five additional rings were installed in a recently formed gap, about 800 m north of the plot. The rings were kept free of seedlings during the study period. The lid was made from the bell-shaped terminal part of the PVC pipe, equipped with gasket to ensure tight sealing. CO₂ concentrations were measured with a diffuse infrared gas analyzer (Vaisala GMP343) installed on the lid with mounting flange. The probe was calibrated with standard CO₂ and pure nitrogen gases, approximately every 6 months. Temperature and relative humidity inside the chamber were measured by a Vaisala HUMICAP. Air inside the chamber was maintained well mixed by a small fan operated at 6 V. To avoid pressure differences between the chamber and the atmosphere, the chamber was vented to the atmosphere through a small hole. CO₂ concentration measurements were recorded by a Vaisala HM70 meter for 5 min at 5 s averaging intervals after closing the chamber. Sampling campaign were conducted at average weekly intervals from June 2013 for a total of 3,847 samples.

2.4 | Flux calculation and data quality check

Soil CO₂ effluxes were calculated from regression of CO₂ concentration within the chamber versus time. For the automated system, effluxes were computed using LI-8100 File Viewer software (version 3.1.0). The software computed the effluxes using the best model between linear and exponential, based on R^2 . Start time was set at 25 s from the time the chamber was closed according to manufacturer recommendation. Values exceeding reasonable limits (0–16 $\mu\text{mol m}^{-2} \text{s}^{-1}$), with $R^2 < 0.97$ or RMSE > 0.2 $\mu\text{mol m}^{-2} \text{s}^{-1}$ were discarded.

For the manual system, effluxes were computed by linear regression using a graphic user interface developed with MATLAB. Linear trends were selected by visual interpretation, by manually setting the

start and end times, which usually implied to discard the first 60 s to ensure that only the linear portion of the curve is used. Values of flux exceeding 16 $\mu\text{mol m}^{-2} \text{s}^{-1}$, and poor good of fitness ($R^2 < 0.9$ or RMSE > 0.2 $\mu\text{mol m}^{-2} \text{s}^{-1}$) were discarded. Other anomalous values were detected by comparing effluxes between consecutive campaigns and discarded if differences between both, previous and following measurements, exceeded 5 $\mu\text{mol m}^{-2} \text{s}^{-1}$.

2.5 | Soil temperature and soil moisture

Continuous soil temperatures were taken in proximity of the automated chambers with four thermistors (model 8150-203, LI-COR) of 6 cm length and were operated in conjunction with the chambers. In January 2016, two soil thermistors (Model 107, Campbell Scientific) of 10.4 cm length were installed permanently and recorded by a datalogger (CR1000, Campbell Scientific) at 5-min interval.

For the manual measurements, soil temperature was taken during four campaigns next to the collars with a platinum thermistor (model HH804U, OMEGA Engineering) inserted at 15 cm of depth.

Soil moisture was monitored by three Time Domain Reflectometers (TDR, Campbell Scientific, CS616) inserted vertically in the soil in proximity of the automated chamber system. Soil moisture measures were taken continuously during the duration of the study. Soil samples were collected between 0 and 15 cm during different soil moisture conditions to calibrate the TDR period against gravimetric measurements. A site specific value of soil bulk density equal 0.75 g/cm^3 was measured by collecting several soil cores with a metallic cylinder of 10.6 cm diameter and 15 cm height. This value was used to transform mass gravimetric measurements to soil volumetric water content.

Other meteorological variables as solar radiation (CMP11, Keep&Zonen), air temperature and relative humidity (HC2S3, Campbell Scientific), and air pressure (pressure transducer mounted on a LI-7550, LiCOR) were obtained from the microclimatic tower located in the plot and used as input variables for the Artificial Neural Network (see below).

2.6 | Forest structure

We recorded the diameter of all the trees at breast height, within 5 m distance from each collar to calculate basal area. We calculated the gap fraction (indirect site fraction) of the canopy above each ring taking hemispherical photographs with a digital camera (Canon EOS 6D, Canon Inc. Japan) provided with a fisheye lens (Sigma 8 mm f/3.5 EX DG Circular Fisheye Lens, Sigma Corporation of America).

2.7 | Statistical analysis

Correlation analysis was used to determinate the relationship between measurements taken by automated and manual chambers, the spatial relationship between temperature and soil CO₂ effluxes and the relationship between the magnitude of rain-induced pulses and soil moisture fluctuations. From the automated time series, ten pulses were selected during the dry seasons and their magnitudes estimated

as the percentage increase between the values of the effluxes immediately before the rain event and at the attained maximum.

A quadratic relationship between spatially averaged soil CO₂ effluxes and soil moisture was fitted using a robust nonlinear least-squares method implemented in the function *fit* (MATLAB 2014a). The relationships were fitted independently for automated and manual samples.

Coefficient of variation (CV), semivariogram (γ), and autocorrelation functions (acf) were used to quantify the temporal and spatial variability of the effluxes during the entire period and during the dry and wet periods separately (for CV and γ only). The autocorrelation as function of time interval τ was defined as:

$$\text{acf}(\tau) = \frac{E[(f(x,t) - \langle f \rangle_t)(f(x,t+\tau) - \langle f \rangle_{t+\tau})]}{\sqrt{E[(f(x,t) - \langle f \rangle_t)^2]} \sqrt{E[(f(x,t+\tau) - \langle f \rangle_{t+\tau})^2]}} \quad (1)$$

where $E[\cdot]$ denotes expectation and $\langle f \rangle_t$ spatial average for all measurements f taken at time t . The semivariogram as function of spatial lag r was defined as:

$$\gamma(r) = E \left[\frac{1}{2} (\bar{f}(x)_T - \bar{f}(x+r)_T)^2 \right] \quad (2)$$

where $\bar{f}(x)_T$ denotes temporal average for measurements at location x across the period T .

Multiway analysis of variance was used to determine the effect on the spatial variability of several factors using the function *anovan* (MATLAB 2014a). The analysis was performed on the residuals between the effluxes and the model with soil moisture fitted in the previous analysis. Significance was determined at $p < .05$.

Diurnal pattern of soil effluxes was computed by averaging continuous measurements as function of time of the day during the 2016 dry season. To compare soil temperature, soil moisture, and soil CO₂ efflux, the diurnal patterns were normalized between 0 and 1.

2.8 | Artificial Neural Networks (ANN)

Because manual and automated measurements were acquired at different temporal resolution and irregular frequency, averaging across space and time is problematic. ANN is a statistical technique commonly used to gap fill biological fluxes (gross primary productivity, ecosystem respiration, and evapotranspiration) obtained from eddy covariance measurements (Papale & Valentini, 2003) in order to produce meaningful time integrated budgets. Here, we used ANN with the same scope. All data were assimilated at daily time step into the ANN which uses meteorological inputs (soil moisture, solar radiation, temperature, and pressure) to predict soil CO₂ effluxes at each location. Once all the series have been put on the same time frame, they were easily averaged.

To train the network, the dataset was randomly divided into a training set (70%), a validation set (15%) and a test set (15%). A two-layer feed-forward network with 10 sigmoid hidden neurons and linear output neurons was trained using the Levenberg-Marquardt algorithm until the mean square error (MSE) of the validation set stop improving (Hagan & Menhaj, 1994). Performance, in term of MSE, was evaluated using the test set at the end of the training. This procedure

was repeated 100 times for each location to produce 100 estimates of daily soil CO₂ effluxes. Training multiple times generates different results due to different initial conditions and random sampling of the three sets. Ensemble at any locations i and day j was obtained as weighted average from the 100 ANN predictions using the inverse of MSE of the test set as weights according to:

$$f_{ij} = \frac{\sum_k f_{ijk}^{\text{ANN}} / \text{MSE}_{ik}}{\sum_k 1 / \text{MSE}_{ik}} \quad (3)$$

The ANN was implemented using the Neural Network Toolbox in MATLAB 2014a.

3 | RESULTS

Time series of soil respiration measurements (Figure 1a,b) showed a clear seasonal pattern in phase with soil moisture (Figure 1c). There was a large spatial variation in the weakly manual measurements and in the four automated measurements. Automated measurements also displayed large temporal variability at finer time scales. Soil CO₂ effluxes ranged from as low as 0.06 to a maximum of 14.07 $\mu\text{mol CO}_2 \text{ m}^{-2} \text{ s}^{-1}$ and 0.25–14.57 $\mu\text{mol CO}_2 \text{ m}^{-2} \text{ s}^{-1}$, for the manual and automated system, respectively.

In addition to seasonal cycle, surface soil moisture exhibited high-frequency fluctuations in correspondence to rain events (Figure 1c). Lower values of soil CO₂ efflux were found when the soil was either dry or completely wet, immediately following heavy rain events in the wet seasons. In contrast, even moderate rain events after long dry spells generated CO₂ pulses of variable magnitude.

Soil temperature exhibited less variation, both diurnal and seasonal, ranging from 22 to 30 degrees Celsius across the entire record. Highest values were reached during the 2016 dry season in correspondence to a strong El Niño event (Figure 1d).

Automated and manual measurements were in good agreement when compared on a daily scale. Figure 2 shows a scatterplot representing the average of the 32 manual measurements for each census against the average of the four chambers during the time of the day correspondent to the duration of the field campaign. Although there was a good correlation ($R^2 = 0.78$, $p < 1 \times 10^{-10}$), manual measurements were higher for low soil CO₂ effluxes and lower for high soil CO₂ effluxes.

Temporal and spatial variabilities of soil respiration were both high with coefficient of variations (CVs) ranging from 0.27 to 0.46, and 0.17 to 0.47 for temporal and spatial CV, respectively (Figure 3a,b). During the dry season, CVs were higher than during the wet season, indicating strong relative variability during low flux periods. Temporal autocorrelation function showed a long-term correlation (>15 months) with annual periodicity (Figure 4c). In contrast no spatial structure was detected in the semivariogram (Figure 3d), suggesting that from a 20 m distance, measurements can be considered statistically independent.

The automated and manual measurements showed a consistent quadratic relationship between soil moisture and soil CO₂ effluxes (Figure 4). For both automated and manual measurements, the peak of soil CO₂ effluxes was at $\sim 0.45 \text{ cm}^3/\text{cm}^3$.

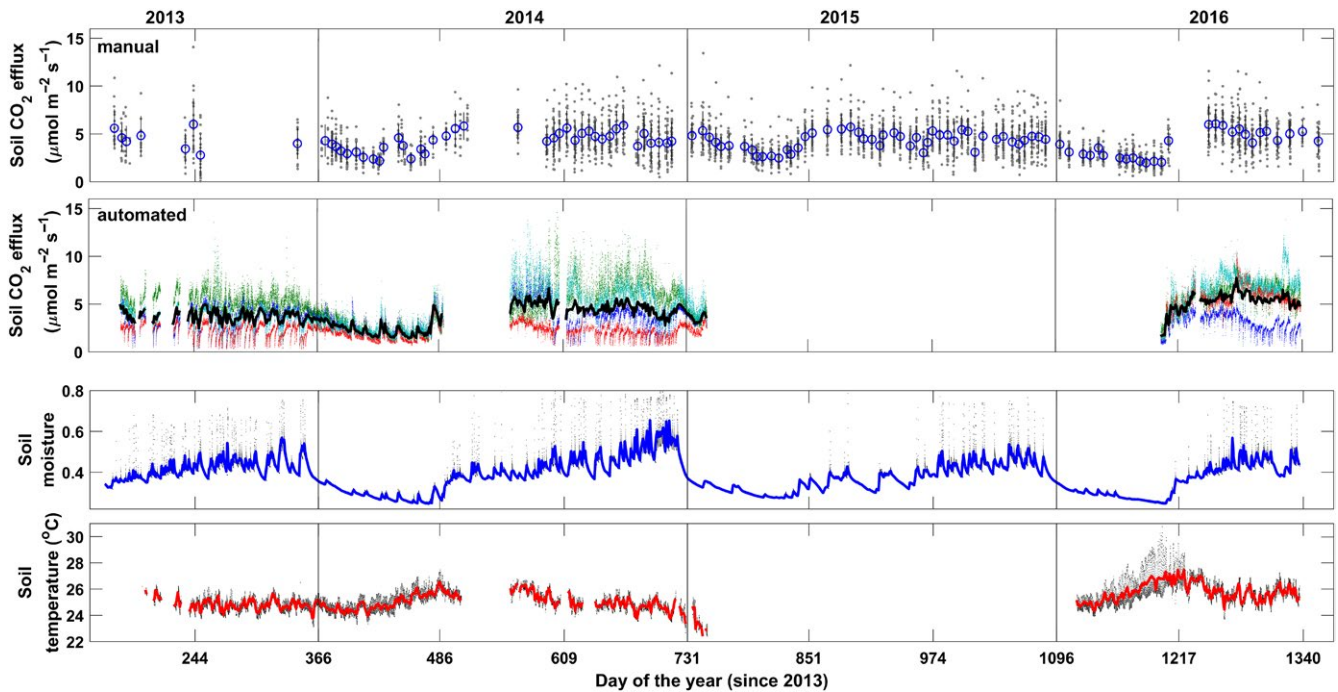


FIGURE 1 Time series of soil respiration (soil CO₂ effluxes) for manual (a), four automated chambers (b), soil moisture (c), and temperature (d) collected on Barro Colorado Island between 2013 and 2016. In (a) points represent single measurements, blue circles field campaign mean, and black lines SE. In b–d) each point indicated an individual measurement, tick lines are daily means. Gaps were due to instrument malfunctioning, lack of personnel, power losses, and maintenance operations

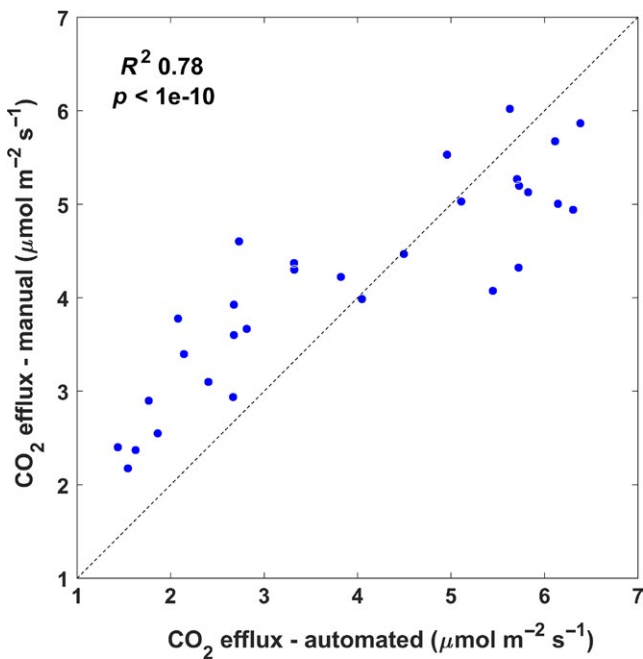


FIGURE 2 Comparison of soil CO₂ efflux measurements estimated as average of four automated chambers and average of 32 manual chambers during periods when both systems were operated. 1:1 line shown for reference

Pulses of soil respiration during dry season were strongly correlated with the magnitude of the soil moisture fluctuations, with the soil CO₂ efflux doubling for a 20% increase in soil moisture (Figure 5).

Automated measurements allowed us to study diurnal cycles in soil respiration, which were consistently detected during the dry seasons with an average amplitude of $\sim 0.6 \mu\text{mol m}^{-2} \text{s}^{-1}$. This diurnal variation was in phase with soil water content, as illustrated in Figure 6, while temperature was lagging for about 5 hr.

Spatial soil temperature variations were minimal, spanning approximately one degree Celsius in each of the four manual censuses (Figure 7). Not surprisingly, these small spatial temperature differences did not explain much variation in the soil CO₂ effluxes. The correlation between manual CO₂ effluxes and soil temperature was significant in one census only ($R^2 = 0.27$, $p = .002$, $n = 32$), marginally significant in one census ($R^2 = 0.10$, $p = .081$, $n = 32$), and not significant in the other two censuses ($R^2 = 0.05$, $p = .219$, $n = 32$; $R^2 = 0$, $p = .861$, $n = 32$). When the significant temperature census was included in the multiway ANOVA, the overall effect of temperature was significant, but mostly in conjunction with gap fraction (Table 2).

Although within topographic features spatial variation was large (coefficient of variation was 20% and 22% along slope and plateau, respectively), the average soil CO₂ efflux along the slope was slightly bigger than on the plateau (4.38 ± 0.07 and $4.22 \pm 0.05 \mu\text{mol m}^{-2} \text{s}^{-1}$, respectively), and the difference was significant ($p < 1 \times 10^{-6}$). However, when topography was included in a multivariate analysis with other variables, only the interaction terms were significant, in particular with basal area and gap fraction (Table 2).

The multiway ANOVA (Table 2) also revealed significant effects of basal area, gap fraction, temperature and several interaction terms that explain spatial variation in the manual measurements after removing

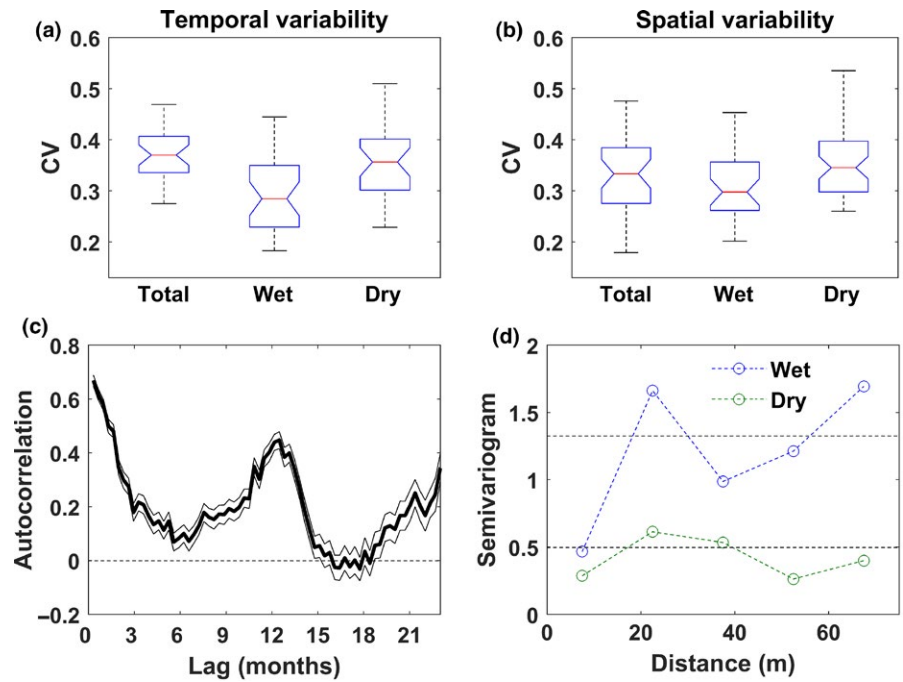


FIGURE 3 Spatiotemporal variation in the manual measurements shows a large degree of variability in both, temporal and spatial axes, strong temporal autocorrelation and lack of spatial structure. Boxplot of coefficient of temporal variation (CV) of soil CO₂ effluxes among locations during all periods, wet (swc > 0.35) and dry (swc < 0.35) conditions (a). Boxplot of coefficient of spatial variation of temporally averaged soil CO₂ effluxes during all period, wet and dry conditions (b). Autocorrelation function (c). Semivariogram during wet and dry conditions (d)

the temporal dependence on soil moisture. However, the total variance explained by the model was only ~13%.

Artificial neural network fits the data reasonably well, with an overall RMSE of 0.74 $\mu\text{mol m}^{-2} \text{s}^{-1}$ ranging from 0.24 to 1.5 depending on locations (Figure 8). The annual (from August to July) integrated soil CO₂ effluxes ($\pm\text{SE}$) were 1,591 (± 61), 1,602 (± 61) and 1,646 (± 57) $\text{gC m}^{-2} \text{year}^{-1}$ for 2013–2014, 2014–2015, and 2015–2016, respectively. Average daily soil CO₂ effluxes were 3.45 (± 0.11) and 4.52 (± 0.19) $\text{gC m}^{-2} \text{day}^{-1}$ during the dry season (January through April) and wet season (May through December), respectively.

4 | DISCUSSION

Our long-term observations displayed large spatial and temporal variability, the latter over a broad range of scales, with similar degree of variation among space and time. Despite lower emissions, the dry season exhibited higher relative variability because dry soil responded

dynamically to rainfall events as commonly observed in water-limited ecosystems (Ma et al., 2012), where they can be responsible for more than 10% of the carbon losses over a year (Jarvis et al., 2007). These temporal processes reflected also on the spatial variability, which was relatively higher during dry season most likely because each location responded differently to these rainy events. Automated measurements showed that soil CO₂ effluxes were greatly reduced immediately following an intense rain event. This effect can last several hours, with a complete recovery of prestorm conditions after approximately 2 days. This means that during the high of the wet season soil respiration is always limited because storm frequency averages one every 2–3 days.

Previous studies highlighted the control of soil moisture on soil respiration (e.g., Davidson et al., 2000; Schwendenmann, Veldkamp, Brenes, O'Brien, & Mackensen, 2003; Sotta et al., 2006; Xu & Qi, 2001). In our study, soil moisture confirmed to be the primary driver of temporal variability in this tropical forest, with temperature playing a secondary role. However, although the effect of soil moisture was

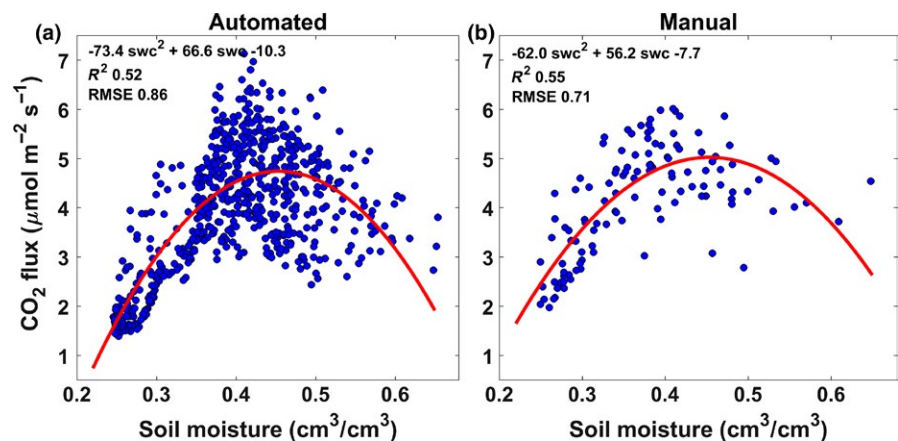


FIGURE 4 Quadratic relationships between soil moisture and soil CO₂ effluxes obtained from automated and manual measurements. Blue dots represent daily average flux measurements with daily averaged soil water content between 0 and 15 cm. Fitted equation, R^2 and root mean square error are also reported

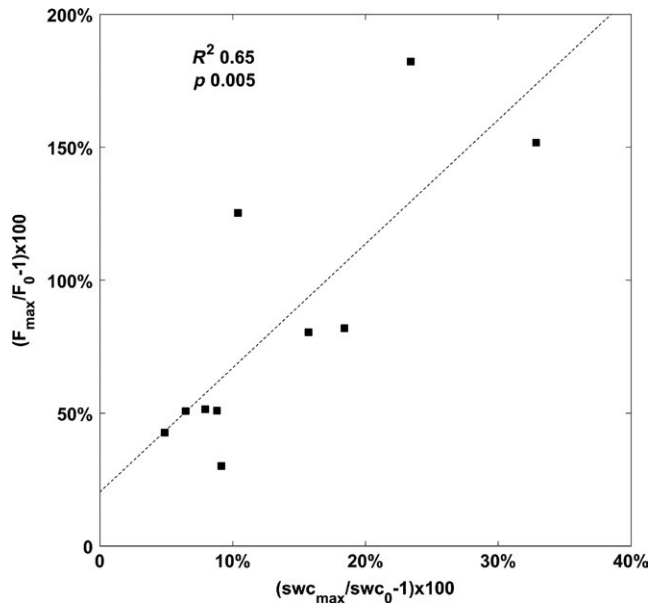


FIGURE 5 Rain-induced pulses of soil CO₂ effluxes (F) explained by relative changes in soil moisture (swc). Each point represents a pulse with magnitude expressed as the relative difference of the flux measured just before the rain event (denoted as 0), and the maximum flux of the pulse (denoted as max). Least-squares line, R^2 and p -value are shown for reference

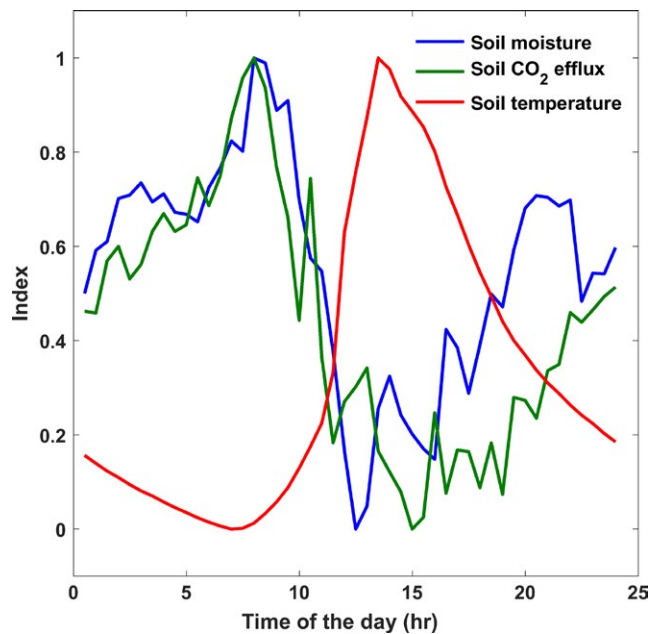


FIGURE 6 Mean diurnal variation of soil CO₂ effluxes is out of phase with soil temperature and soil moisture during 2016 dry season. All variables are normalized between 0 and 1 for comparison

well described by a quadratic relationship, large scatter still remains at intermediate moisture conditions, evident from the automated measurements which have higher temporal resolution and a better representation of the rain pulses. The soil CO₂ effluxes peak, at 0.45 cm³/cm³, was consistent with other studies that have used a parabolic function to describe the relationship between soil moisture and soil

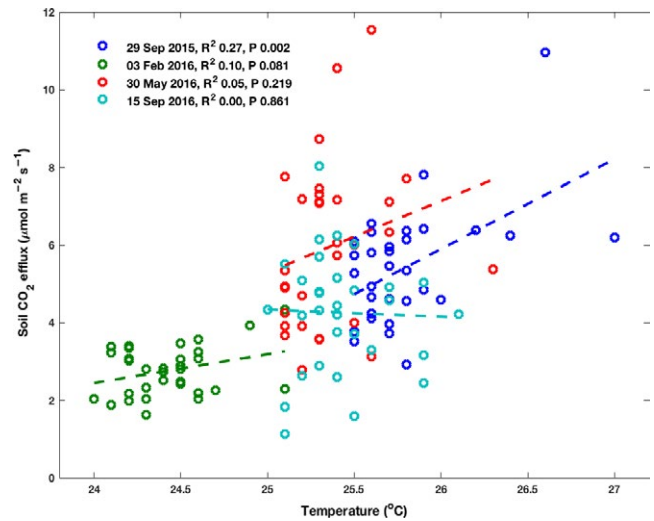


FIGURE 7 Relationship between manual CO₂ effluxes and soil temperature measured in the proximity of the collars during four filed campaigns. Date of the census, R^2 and p -value are indicated in the legend. Linear regressions are indicated by dashed lines for reference

respiration (e.g., Chambers et al., 2004; Sotta et al., 2004). For example, Wood et al. (2013) found higher soil CO₂ efflux at 0.375 m³/m³, and Schwendenmann et al. (2003) found that the peak ranged from 0.35 to 0.50 m³/m³ depending upon the type of soil.

In tropical forests, where temperature variations, both temporal and spatial, are generally small, soil temperature does not significantly influence soil respiration. Actually, the time series displayed an apparent negative correlation (Figure 1). This confounding effect, analogous to what was found by Davidson et al. (1998), is caused by soil moisture to mask the effect of temperature, because the covariation between cold/hot and wet/dry conditions.

In fact, the largest fluctuations in soil temperature were observed during the dry season. In this period, clear sky conditions and canopy opening left by the dry deciduous species, allow larger amounts of solar radiation to reach the forest floor, generating deep diurnal cycles in soil heat. It is in concomitance with these fluctuations that flux measurements showed a detectable diurnal cycle (Figure 7). An in-depth analysis of the lags between temperature and soil CO₂ effluxes demonstrated that these cycles were not consistent with a temperature dependent process, because effluxes peaked at 8:00 a.m. while temperature peaked at 13:30 p.m. Considering that gas soil diffusivity is relatively high in dry conditions, it seems unlikely that temperature produced a lagged response of more than 18 hr.

Again, this diurnal pattern is almost in phase with soil moisture, which in the dry season also exhibited detectable diurnal cycles generated by root water uptake. This suggests two possible explanations: (1) Sugars are synthesized during the day and translocated to roots. These sugars are respired by roots or released as exudates in the rhizosphere, and used by soil microorganisms such as mycorrhizae (Kuzakov & Gavrichkova, 2010). The time of this coupling, which is determined by phloem transport dynamics (Mencuccini & Hölttä, 2010), generates a lagged response between photosynthesis (or transpiration) and soil respiration. (2) Part of the carbon respired by roots can be transported

TABLE 2 Multiway analysis of variance (ANOVA) for testing the effects of multiple factors and their interactions on the mean of the residual soil CO₂ effluxes (after removing the temporal dependence on soil moisture with a quadratic model)

Variable	Explained variance (%)	Coefficient ^a	F-statistics	p-value
Top	0.06	–	2.23	.1358
BA	4.92	0.528	194	<1 × 10 ⁻¹⁰
GF	1.65	0.927	65	<1 × 10 ⁻¹⁰
Temp	0.58	0.480	22.75	<1 × 10 ⁻⁵
Top*BA	5.53	–	217.87	<1 × 10 ⁻¹⁰
Top*GF	0.18	–	7.08	.0078
Top*Temp	0.06	–	2.39	.1222
BA*GF	0.41	-0.192	16.34	<1 × 10 ⁻⁴
BA*Temp	0.28	0.157	10.94	<1 × 10 ⁻⁴
GF*Temp	4.25	-0.257	167.4	<1 × 10 ⁻¹⁰
Total	12.97			

Top: plateau and slope, BA, log of basal area within 5 m from the collar; GF, gap fraction from hemispherical photos; Temp, soil temperature measured on 29 Sept 2015. All continuous variables are rescaled to unit variance.

^aFor continuous variables only.

aboveground through the xylem rather than being diffused through the soil (Aubrey & Teskey, 2009), reducing measured soil CO₂ effluxes during periods of high transpiration. Although this pattern was extremely interesting, the magnitude of the fluctuations was relatively small, and the phenomenon was present only during dry periods, with marginal contribution for annual budgets. For this reason, it was neglected for upscaling manual measurements.

We did not find spatial correlation in our sampling design, which might indicate a lack of large-scale structure, confirmed by the weak effect of topography. This simplified the analyses because the samples could be considered statistically independent. However, it does not shed light on the spatial scales of variation and the possible mechanisms that generated such variation, suggesting a presence of an unresolved fine scale variability, which might be much smaller than our sparse (20 m × 20 m) sampling design, as previously observed by Kursar (1989).

Although spatial variability was less characterized than temporal variability, our study suggests that forest structure has important direct and indirect influences. For example, the effect of temperature was small but significant, as indicated by the multiway ANOVA, but it was the interactions between temperature and gap fraction that

explained most of the variance. This suggests that spatial temperature effects were mediated by canopy structure, which may prove important for upscaling soil CO₂ effluxes using remote sensing products such as LiDAR. Similarly, higher soil CO₂ effluxes were observed from slope compared to plateau, a topographic effect generally attributed to hydrological processes related to water transport and drainage (Epron et al., 2006; Ngo et al., 2013; Zhou et al., 2016). However, the multiway ANOVA showed that the topographic effect was mostly significant when interacting with basal area. This might be consistent with the observation that within these forests, mean canopy height, a predictor of above ground biomass, is strongly correlated with hydrological terrain attributes, with taller forests in the proximity of the drainage network (Detto, Muller-Landau, Mascaro, & Asner, 2013).

Other studies investigated the spatial correlation between the soil CO₂ efflux and tree proximity, but results were not consistent and the mechanisms unclear. For example, Sotta et al. (2004) found no correlation with basal area. Similarly, Bréchet, Ponton, Alméras, Bonal, and Epron (2011) showed that the soil CO₂ efflux was poorly explained by forest structure because the contribution of trees to soil functioning depends on both, their quantitative characteristics and qualitative

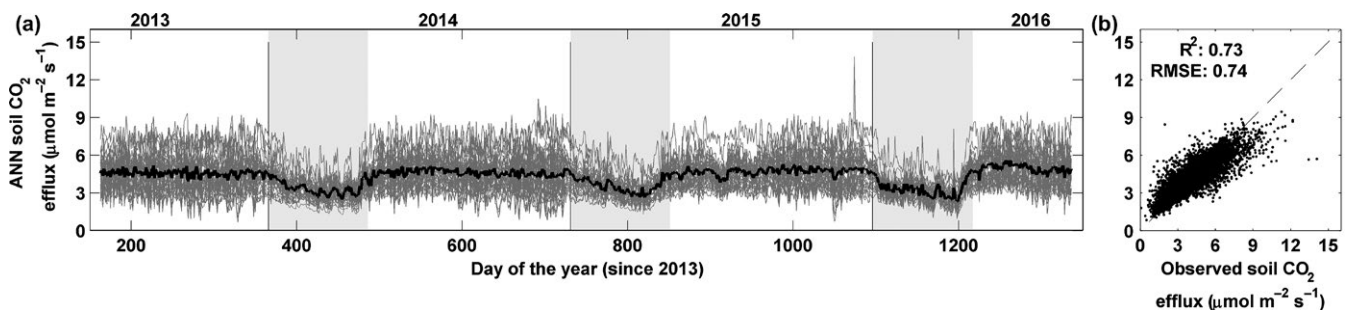


FIGURE 8 (a) Ensemble ANN predictions at daily time step for each location (gray lines). Tick black line is the average across the 36 locations (32 manual and 4 automated), gray shaded areas indicate dry seasons. (b) Comparison between observed and simulated effluxes. R^2 , root mean square error and 1:1 line are given for reference

traits. Conversely, Shibistova et al. (2002) found that rates from relatively open areas were about half of those observed below or around trees, a result that was attributed mostly to root density. Vargas and Allen (2008) found that gaps in the canopy could explain fluctuations in soil volumetric water content, causing soils to become wetter or drier faster during or after a rain event, respectively. Strong correlation with forest stand structure at ecosystem scale was also found by Katayama et al. (2009) and Shi, Gao, Cai, and Jin (2016).

The study period was characterized by an ENSO cycle that culminated with a strong El Niño in 2015–2016. During El Niño, this region of the tropics experiences relatively dry and warm conditions. Because the relationship between soil respiration and soil moisture is not monotonic, dry conditions can enhance or reduce annual carbon losses. Our study indicated an increase of annual CO₂ fluxes during El Niño, mainly driven by a reduction in the frequency of saturated water soil conditions during the wet season. Considering that the frequency and intensity of ENSO are predicted to increase, these results will be useful to understand the impact of climate change on tropical forest carbon cycle.

This study showed how an innovative combination of long-term automated and manual measurements could help to better quantify soil CO₂ effluxes in a temporally and spatially variable environment and provide an accurate estimation of landscape soil carbon losses at annual scale. Our soil CO₂ effluxes fall within the range of the tropical studies presented in Table 1. The annual budget is not statistically different from the mean of the distribution computed from the averaged effluxes reported in these studies (*p*-value .1608, *t*-test with 48 dof). However, the length of the study period and the method used for measuring the soil CO₂ effluxes varies among studies, making meaningful comparison difficult, highlighting the importance of long-term observations, and standardized method.

Statistical models as the ANN implemented in this study are useful tools to integrate the measurements in space and time, but mechanistic models will be necessary to project soil carbon losses from tropical forests under different climate change scenarios. For this reason, it is essential that future research aims to understand some of the unresolved variability of soil respiration, especially the spatial variability. Important mechanisms that should receive better attention in tropical forests are ecological drivers, as the carbon translocation from above ground to roots and the interactions with soil microorganisms.

ACKNOWLEDGEMENTS

Financial support from ForestGEO-CTFS of the Smithsonian Tropical Research Institute. We thank E. Sayer and R. Pinzon for their support with the automated systems, P. Ramos, P. Villareal, E. Diaz, and F. Protti for field assistance and all the BCI staff for logistical support.

CONFLICT OF INTEREST

None declared.

REFERENCES

- Adachi, M., Bekku, Y. S., Konuma, A., Kadir, W. R., Okuda, T., & Koizumi, H. (2005). Required sample size for estimating soil respiration rates in large areas of two tropical forests and of two types of plantation in Malaysia. *Forest Ecology and Management*, 210, 455–459.
- Adachi, M., Bekku, Y. S., Rashidah, W., Okuda, T., & Koizumi, H. (2006). Differences in soil respiration between different tropical ecosystems. *Applied Soil Ecology*, 34, 258–265.
- Adachi, M., Ishida, A., Bunyavejchewin, S., Okuda, T., & Koizumi, H. (2009). Spatial and temporal variation in soil respiration in a seasonally dry tropical forest, Thailand. *Journal of Tropical Ecology*, 25, 531–539.
- Aubrey, D. P., & Teskey, R. O. (2009). Root-derived CO₂ efflux via xylem stream rivals soil CO₂ efflux. *New Phytologist*, 184, 35–40.
- Baillie, I., Elsenbeer, H., Barthold, F., Grimm, R., & Stallard, R. (2005). *Semi-detailed soil survey of Barro Colorado Island, Panama*. PhD Proposal, 1
- Balogh, J., Pinter, K., Foti, Sz, Cserhalmi, D., Papp, M., & Nagy, Z. (2011). Dependence of soil respiration on soil moisture, clay content, soil organic matter, and CO₂ uptake in dry grasslands. *Soil Biology and Biochemistry*, 43, 1006–1013.
- Barberán, A., McGuire, K. L., Wolf, J. A., Jones, F. A., Wright, S. J., Turner, B. L., ... Fierer, N. (2015). Relating belowground microbial composition to the taxonomic, phylogenetic, and functional trait distributions of trees in a tropical forest. *Ecology Letters*, 18, 1397–1405.
- Bardgett, R. D., Freeman, C., & Ostle, N. J. (2008). Microbial contributions to climate change through carbon cycle feedbacks. *The ISME Journal*, 2, 805–814.
- Beer, C., Reichstein, M., Tomelleri, E., Ciais, P., Jung, M., Carvalhais, N., ... Papale, D. (2010). Terrestrial gross carbon dioxide uptake: Global distribution and covariation with climate. *Science*, 329, 834–839.
- Bréchet, L., Ponton, S., Alméras, T., Bonal, D., & Epron, D. (2011). Does spatial distribution of tree size account for spatial variation in soil respiration in a tropical forest? *Plant and Soil*, 347, 293–303.
- Cavaleri, M. A., Reed, S. C., Smith, W. K., & Wood, T. E. (2015). Urgent need for warming experiments in tropical forests. *Global Change Biology*, 21, 2111–2121.
- Chambers, J. Q., Tribuzy, E. S., Toledo, L. C., Crispim, B. F., Higuchi, N., Dos Santos, J., ... Trumbore, S. E. (2004). Respiration from a tropical forest ecosystem: Partitioning of sources and low carbon use efficiency. *Ecological Applications*, 14, 72–88.
- Cleveland, C. C., & Townsend, A. R. (2006). Nutrient additions to a tropical rain forest drive substantial soil carbon dioxide losses to the atmosphere. *Proceedings of the National Academy of Sciences of the United States of America*, 103, 10316–10321.
- Cook, F. J., & Orchard, V. A. (2008). Relationships between soil respiration and soil moisture. *Soil Biology and Biochemistry*, 40, 1013–1018.
- Cox, P. M., Pearson, D., Booth, B. B., Friedlingstein, P., Huntingford, C., Jones, C. D., & Luke, C. M. (2013). Sensitivity of tropical carbon to climate change constrained by carbon dioxide variability. *Nature*, 494, 341–344.
- Davidson, E. A., Belk, E., & Boone, R. D. (1998). Soil water content and temperature as independent or confounded factors controlling soil respiration in a temperate mixed hardwood forest. *Global Change Biology*, 4, 217–227.
- Davidson, E. A., Samanta, S., Caramori, S. S., & Savage, K. (2012). The Dual Arrhenius and Michaelis-Menten kinetics model for decomposition of soil organic matter at hourly to seasonal time scales. *Global Change Biology*, 18, 371–384.
- Davidson, E. A., Verchot, L. V., Cattaneo, J. H., Ackerman, I. L., & Carvalho, J. E. M. (2000). Effects of soil water content on soil respiration in forests and cattle pastures of eastern Amazonia. *Biogeochemistry*, 48, 53–69.
- Detto, M., Molini, A., Katul, G., Stoy, P., Palmroth, S., & Baldocchi, D. (2012). Causality and persistence in ecological systems: A nonparametric spectral granger causality approach. *The American Naturalist*, 179, 524–535.

- Detto, M., Muller-Landau, H. C., Mascaró, J., & Asner, G. P. (2013). Hydrological networks and associated topographic variation as templates for the spatial organization of tropical forest vegetation. *PLoS One*, 8(10), e76296.
- Epron, D., Bosc, A., Bonal, D., & Freycon, V. (2006). Spatial variation of soil respiration across a topographic gradient in a tropical rain forest in French Guiana. *Journal of Tropical Ecology*, 22, 565–574.
- Fang, C., & Moncrieff, J. B. (1999). A model for soil CO₂ production and transport 1: Model development. *Agricultural and Forest Meteorology*, 95, 225–236.
- Fernandes, S. A. P., Bernoux, M., Cerri, C. C., Feigl, B. J., & Piccolo, M. C. (2002). Seasonal variation of soil chemical properties and CO₂ and CH₄ fluxes in unfertilized and P-fertilized pastures in an Ultisol of the Brazilian Amazon. *Geoderma*, 107, 227–241.
- Giardina, C. P., Litton, C. M., Crow, S. E., & Asner, G. P. (2014). Warming-related increases in soil CO₂ efflux are explained by increased below-ground carbon flux. *Nature Climate Change*, 14, 822–827.
- Goulden, M. L., Munger, J. W., Fan, S.-M., Daube, B. C., & Wofsy, S. C. (1996). Measurements of carbon sequestration by long-term eddy covariance: Methods and a critical evaluation of accuracy. *Global Change Biology*, 2, 169–182.
- Hagan, M. T., & Menhaj, M. (1994). Training feedforward networks with the Marquardt algorithm. *IEEE Transactions on Neural Networks*, 5, 989–993.
- Hanson, P. J., Wullschlegel, S. D., Bohlman, S. A., & Todd, D. E. (1993). Seasonal and topographic patterns of forest floor CO₂ efflux from an upland oak forest. *Tree Physiology*, 13, 1–15.
- Hashimoto, S., Tanaka, N., Suzuki, M., Inoue, A., Takizawa, H., Kosaka, I., ... Tangtham, N. (2004). Soil respiration and soil CO₂ concentration in a tropical forest, Thailand. *Journal of Forest Research*, 9, 75–79.
- Houghton, R. A. (2005). Aboveground forest biomass and the global carbon balance. *Global Change Biology*, 11, 945–958.
- Ibañez, T. S. (2015). *Soil respiration in primary and secondary tropical Montane rain forest*. (Master of Science Thesis), Gothenburg, Sweden: University of Gothenburg.
- Jarvis, P., Rey, A., Petsikos, C., Wingate, L., Rayment, M., Pereira, J., ... Valentini, R. (2007). Drying and wetting of Mediterranean soils stimulates decomposition and carbon dioxide emission: The Birch effect. *Tree Physiology*, 27(7), 929–940.
- Jiang, L., Ma, S., Zhou, Z., Zheng, T., Jiang, X., Cai, Q., ... Fang, J. (2016). Soil respiration and its partitioning in different components in tropical primary and secondary mountain rain forests in Hainan Island, China. *Journal of Plant Ecology*, rtw080, 1–9.
- Jobbágy, E. G., & Jackson, R. B. (2000). The vertical distribution of soil organic carbon and its relation to climate and vegetation. *Ecological Applications*, 10(2), 423–436.
- Katayama, A., Kume, T., Komatsu, H., Ohashi, M., Nakagawa, M., Yamashita, M., ... Kumagai, T. (2009). Effect of forest structure on the spatial variation in soil respiration in a Bornean tropical rainforest. *Agricultural and Forest Meteorology*, 149, 1666–1673.
- Kiese, R., & Butterbach-Bahl, K. (2002). N₂O and CO₂ emissions from three different tropical forest sites in the wet tropics of Queensland, Australia. *Soil Biology and Biochemistry*, 34, 975–987.
- Kosugi, Y., Mitani, T., Itoh, M., Noguchi, S., Tani, M., Matsuo, N., ... Nik, A. R. (2007). Spatial and temporal variation in soil respiration in a Southeast Asian tropical rainforest. *Agricultural & Forest Meteorology*, 147, 35–47.
- Kursar, T. A. (1989). Evaluation of soil respiration and soil CO₂ concentration in a lowland moist forest in Panama. *Plant and Soil*, 29, 21–29.
- Kuzakov, Y., & Gavrishkova, O. (2010). Time lag between photosynthesis and carbon dioxide efflux from soil: A review of mechanisms and controls. *Global Change Biology*, 16, 3386–3406.
- La Scala, N., Marques, J., Pereira, G. T., & Corá, J. E. (2000). Carbon dioxide emission related to chemical properties of a tropical bare soil. *Soil Biology & Biochemistry*, 32, 1469–1473.
- Leigh, E. G. Jr, Loo de Lao, S., Condit, R., Hubbell, S. P., Foster, R. B., & Perez, R. (2004). In E. C. Losos, J. Leigh, & Egbert Giles (Eds.), *Tropical forest diversity and dynamism: Findings from a large-scale plot network* (pp. 451–463). Chicago: University of Chicago Press.
- Li, Y., Xu, M., & Zou, X. (2006). Heterotrophic soil respiration in relation to environmental factors and microbial biomass in two wet tropical forests. *Plant and Soil*, 281, 193–201.
- Li, P., Yang, Y., & Fang, J. (2013). Variations of root and heterotrophic respiration along environmental gradients in China's forests. *Journal of Plant Ecology*, 6(5), 358–367.
- Linn, D. M., & Doran, J. W. (1984). Effect of water-filled pore space on carbon dioxide and nitrous oxide production in tilled and nontilled soils. *Soil Science Society of America Journal*, 48, 1267–1272.
- Liptzin, D., Silver, W. L., & Detto, M. (2010). Temporal dynamics in soil oxygen and greenhouse gases in two humid tropical forests. *Ecosystems*, 14, 171–182.
- Lükewille, A., & Wright, R. F. (1997). Experimentally increased soil temperature causes release of nitrogen at a boreal forest catchment in southern. *Global Change Biology*, 3, 13–21.
- Ma, S., Baldocchi, D. D., Hatala, J. A., Detto, M., & Yuste, J. C. (2012). Are rain-induced ecosystem respiration pulses enhanced by legacies of antecedent photodegradation in semi-arid environments? *Agricultural and Forest Meteorology*, 154, 203–213.
- Malhi, Y., Doughty, C., & Galbraith, D. (2011). The allocation of ecosystem net primary productivity in tropical forests. *Philosophical Transactions of the Royal Society B: Biological Sciences*, 366, 3225–3245.
- Malhi, Y., Nobre, A. D., Grace, J., Kruijt, B., Pereira, M. G. P., Culf, A., & Scott, S. (1998). Carbon dioxide transfer over a Central Amazonian rain forest. *Journal of Geophysical Research*, 103, 31593–31612.
- Mencuccini, M., & Hölttä, T. (2010). The significance of phloem transport for the speed with which canopy photosynthesis and belowground respiration are linked. *New Phytologist*, 185, 189–203.
- Metcalfe, D. B., Meir, P., Aragao, L. E. O. C., Malhi, Y., da Costa, A. C. L., Braga, A., ... Williams, M. (2007). Factors controlling spatio-temporal variation in carbon dioxide efflux from surface litter, roots, and soil organic matter at four rain forest sites in the eastern Amazon. *Journal of Geophysical Research*, 112, G04001.
- Mo, J., Zhang, W., Zhu, W., Gundersen, P., Fang, Y., Li, D., & Wang, H. (2008). Nitrogen addition reduces soil respiration in a mature tropical forest in southern China. *Global Change Biology*, 14, 403–412.
- Ngo, K. M., Turner, B. L., Muller-Landau, H. C., Davies, S. J., Larjavaara, M., bin Nik Hassan, N. F., & Lum, S. (2013). Carbon stocks in primary and secondary tropical forests in Singapore. *Forest Ecology and Management*, 296, 81–89.
- Ohashi, M., Kume, T., Yamane, S., & Suzuki, M. (2007). Hot spots of soil respiration in an Asian tropical rainforest. *Geophysical Research Letters*, 34, 2–5.
- Pan, Y., Birdsey, R. A., Fang, J., Houghton, R., Kauppi, P. E., Kurz, W. A., ... Hayes, D. (2011). A large and persistent carbon sink in the world's forests. *Science*, 333, 988–993.
- Papale, D., & Valentini, R. (2003). A new assessment of European forests carbon exchanges by eddy fluxes and artificial neural network spatialization. *Global Change Biology*, 9, 525–535.
- Pendall, E., Bridgman, S., Hanson, P. J., Hungate, B., Kicklighter, D. W., Johnson, D. W., ... Wan, S. (2004). Below-ground process responses to elevated CO₂ and temperature: A discussion of observations, measurement methods, and models. *New Phytologist*, 162, 311–322.
- Phillips, C. L., Bond-Lamberty, B., Desai, A. R., Lavoie, M., Risk, D., Tang, J., ... Vargas, R. (2017). The value of soil respiration measurements for interpreting and modeling terrestrial carbon cycling. *Plant and Soil*, 413, 1–25.
- Raich, J. W., & Schlesinger, W. H. (1992). The global carbon dioxide flux in soil respiration and its relationship to vegetation and climate. *Tellus*, 44B, 81–89.
- Raich, J. W., & Tufekcioglu, A. (2000). Vegetation and soil respiration: Correlations and controls. *Biogeochemistry*, 48, 71–90.

- Sayer, E. J., Heard, M. S., Grant, H. K., Marthews, T. R., & Tanner, E. V. J. (2011). Soil carbon release enhanced by increased tropical forest litter-fall. *Nature Climate Change*, *1*, 304–307.
- Schwendenmann, L., & Veldkamp, E. (2006). Long-term CO₂ production from deeply weathered soils of a tropical rain forest: Evidence for a potential positive feedback to climate warming. *Global Change Biology*, *12*, 1878–1893.
- Schwendenmann, L., Veldkamp, E., Brenes, T., O'Brien, J. J., & Mackensen, J. (2003). Spatial and temporal variation in soil CO₂ efflux in an old-growth neotropical rain forest, La Selva, Costa Rica. *Biogeochemistry*, *64*, 111–128.
- Sha, L., Zheng, Z., Tang, J., Wang, Y., Zhang, Y., Cao, M., ... Sun, Y. (2005). Soil respiration in tropical seasonal rain forest in Xishuangbanna, SW China. *Science in China Series D Earth Sciences*, *48*, 189–197.
- Shi, B., Gao, W., Cai, H., & Jin, G. (2016). Spatial variation of soil respiration is linked to the forest structure and soil parameters in an old-growth mixed broadleaved-Korean pine forest in northeastern China. *Plant and Soil*, *400*, 263–274.
- Shibistova, O., Lloyd, J., Evgrafova, S., Savushkina, N., Zrazhevskaya, G., Arneith, A., ... Dettlfeuschulze, E. (2002). Seasonal and spatial variability in soil CO₂ efflux rates for a central Siberian *Pinus sylvestris* forest. *Tellus Series B-Chemical and Physical Meteorology*, *54B*, 552–567.
- Silver, W. L., Scatena, F. N., Johnson, A. H., Siccama, T. G., & Sanchez, M. J. (1994). Nutrient availability in a montane wet tropical forest: Spatial patterns and methodological considerations. *Plant and Soil*, *164*, 129–145.
- Sotta, E. D. (1998). *Fluxo De CO₂ Entre Solo E Atmosfera Em Floresta Tropical Úmida Da Amazônia Central*, Programa de Pós-graduação em Biologia Tropical e Recursos Naturais do convênio INPA/UA.
- Sotta, E. D., Meir, P., Malhi, Y., Nobre, A. D., Hodnett, M., & Grace, J. (2004). Soil CO₂ efflux in a tropical forest in the Central Amazon. *Global Change Biology*, *10*, 601–617.
- Sotta, E. D., Veldkamp, E., Guimaraes, B. R., Paixao, R. K., Ruivo, M. L. P., & Almeida, S. S. (2006). Landscape and climatic controls on spatial and temporal variation in soil CO₂ efflux in an Eastern Amazonian Rainforest, Caxiuana, Brazil. *Forest Ecology and Management*, *237*, 57–64.
- Takahashi, M., Hirai, K., Limtong, P., Leaugvutivirog, C., Panuthai, S., Suksawang, S., ... Marod, D. (2011). Topographic variation in heterotrophic and autotrophic soil respiration in a tropical seasonal forest in Thailand. *Soil Science and Plant Nutrition*, *57*, 452–465.
- Trumbore, S. (2006). Carbon respired by terrestrial ecosystems—recent progress and challenges. *Global Change Biology*, *12*, 141–153.
- Valentini, C. M. A., Sanches, L., de Paula, S. R., Vourlitis, G. L., de Souza Nogueira, J., Pinto Jr., O. B., & de Almeida Lobo, F. (2008). Soil respiration and aboveground litter dynamics of a tropical transitional forest in north-west Mato Grosso, Brazil. *Journal of Geophysical Research*, *113*, G00B10.
- Vargas, R., & Allen, M. F. (2008). Diel patterns of soil respiration in a tropical forest after Hurricane Wilma. *Journal of Geophysical Research: Biogeosciences*, *113*(G03021), 1–10.
- Vargas, R., Detto, M., Baldocchi, D. D., & Allen, M. F. (2010). Multiscale analysis of temporal variability of soil CO₂ production as influenced by weather and vegetation. *Global Change Biology*, *16*, 1589–1605.
- Weintraub, S. R., Taylor, P. G., Porder, S., Cleveland, C. C., Asner, G. P., & Townsend, A. R. (2015). Topographic controls on soil nitrogen availability in a lowland tropical forest. *Ecology*, *96*(6), 1561–1574.
- Windsor, D. M. (1990). Climate and moisture variability in a tropical forest: Long-term records from Barro Colorado Island, Panama. *Smithsonian Contributions to the Earth Sciences*, *29*, 1–145.
- Wofsy, S. C., Goulden, M. L., Munger, J. W., Fan, S. M., Bakwin, P. S., Daube, B. C., ... Bazzaz, F. A. (1993). Net exchange of CO₂ in a mid-latitude forest. *Science*, *260*, 1314–1317.
- Wood, T. E., Detto, M., & Silver, W. L. (2013). Sensitivity of soil respiration to variability in soil moisture and temperature in a humid tropical forest. *PLoS One*, *8*(12), e80965.
- Wu, J., Goldberg, S. D., Mortimer, P. E., & Xu, J. (2016). Soil respiration under three different land use types in a tropical mountain region of China. *Journal of Mountain Science*, *13*, 416–423.
- Xu, M., & Qi, Y. (2001). temperature are negatively correlated through a simple linear relationship with R² values moisture are positively correlated with R² values Q₁₀. *Global Biogeochemical Cycles*, *15*(3), 687–696.
- Zhou, W.-J., Lu, H.-Z., Zhang, Y.-P., Sha, L.-Q., Schaefer, D. A., Song, Q.-H., ... Deng, X.-B. (2016). Hydrologically transported dissolved organic carbon influences soil respiration in a tropical rainforest. *Biogeosciences*, *13*, 5487–5497.
- Zhou, Z., Jiang, L., Du, E., Hu, H., Li, Y., Chen, D., & Fang, J. (2013). Temperature and substrate availability regulate soil respiration in the tropical mountain rainforests, Hainan Island, China. *Journal of Plant Ecology*, 1–10.

SUPPORTING INFORMATION

Additional Supporting Information may be found online in the supporting information tab for this article.

How to cite this article: Rubio VE, Detto M. Spatiotemporal variability of soil respiration in a seasonal tropical forest. *Ecol Evol*. 2017;7:7104–7116. <https://doi.org/10.1002/ece3.3267>